

Chapter 4

PHY Layer Issues – Spatial Processing

A wireless modem equipped with multiple antennas is capable of exploiting the spatial diversity of wireless channels. The *space domain* enabled by the antenna array introduces an additional dimension to the time-frequency radio resource. Through space-time processing, an antenna array can improve key operational parameters such as the SINR, the data rate, and the outage probability over a single antenna wireless system. Other major benefits of spatial processing include

- better interference/jammer rejection
- higher power efficiency
- lower cost, distributed hardware

Antenna array technology encompasses a wide variety of techniques that can be used at both the base-station and in the user terminal. There are two main classes of spatial processing techniques, namely, *beamforming* and *space-time coding*. Early beamforming techniques are *SINR-oriented*, involving linear combining of transmit and received signals from multiple antennas. The main objective is to maximize the instantaneous signal-to-interference-and-noise ratio (SINR). More recent techniques, such as space-time coding, are mostly *diversity-and-efficiency-oriented*, focusing on lowering the BER of a high-speed link over fading channels. As will be shown in the ensuing discussion, these two types of techniques can be synergistically combined for broadband OFDM systems.

4.1 Antenna array fundamentals

To better understand the principles of array processing, consider the scenario depicted in Figure 4.1 where a narrowband signal $s(t)e^{j\omega_0 t}$ impinges on an array

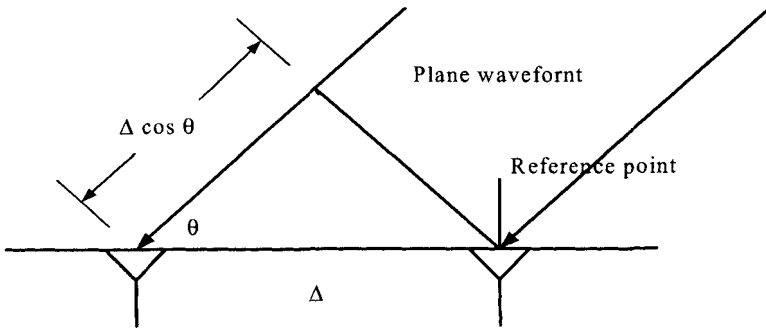


Figure 4.1: A 2-element array and its response to narrowband signal

of two elements from angle θ . The carrier frequency of the narrow band signal is ω_0 , and the spacing between the two antenna elements is Δ .

From the figure, it can be seen that the propagation delay between the first and second antenna elements is

$$\tau = \frac{\Delta \cos \theta}{c}$$

where c is the speed of light. $\omega_0 = 2\pi c/\lambda$. Consequently, the carrier phase shift between the two antenna element is given by

$$\phi = \omega_0 \tau = \omega_0 \frac{\Delta \cos \theta}{c} = \frac{2\pi \Delta \cos \theta}{\lambda}.$$

Putting the two *baseband* array outputs in vector form, we have

$$\begin{aligned} \mathbf{y}(t) &= [y_1(t) \quad y_2(t)]^T = [s(t) \quad s(t - \tau)]^T \\ &= [1 \quad e^{-j \frac{2\pi \Delta \cos \theta}{\lambda}}]^T s(t) = \mathbf{a}(\theta) s(t). \end{aligned} \quad (4.1)$$

An important assumption we invoked here is that the signal is *narrow-band* and therefore the propagation delay between antennas, τ , is insignificant relative to the coherence time of the signal. In other words, $s(t)$ can be regarded as a constant over the period τ . (4.1) can be easily extended to cases with M ($M > 2$) receiving antennas:

$$\begin{aligned} \mathbf{y}(t) &= \left[1 \quad e^{-j \frac{2\pi \Delta \cos \theta}{\lambda}} \quad \dots \quad e^{-j \frac{2\pi \Delta(M-1) \cos \theta}{\lambda}} \right]^T s(t) \\ &= \mathbf{a}(\theta) s(t). \end{aligned} \quad (4.2)$$

The above $\mathbf{a}(\theta)$ is termed as the *steering vector* - it is a function of the angle-of-arrival (AOA) and the array configuration. With only one path between the source (e.g., the user) and the array (e.g., the base-station), the array response vector is identical to the steering vector up to a complex scalar.

In most practical situations with multipath reflections, the antenna output vector is the superposition of these multipath signals:

$$\mathbf{y}(t) = \sum_{l=1}^L \nu_l \mathbf{a}(\theta_l) s_l(t) = \mathbf{a}s(t) \quad (4.3)$$

where L denotes the total number of coherent paths, and ν_l represents the complex gain from direction θ_l . The composite channel response, \mathbf{a} , termed as the *spatial signature* (SS), characterizes the spatial propagation channel between the transmitter and the receiver antenna array.

For a multiuser system with additional noise, the array output can be written as

$$\begin{aligned} \mathbf{y}(t) &= \sum_{i=1}^P \mathbf{a}_i s_i(t) + \mathbf{n}(t) \\ &= \mathbf{A}s(t) + \mathbf{n}(t) \\ \mathbf{A} &= [\mathbf{a}_1 \quad \mathbf{a}_2 \quad \cdots \quad \mathbf{a}_P] \\ \mathbf{s}(t) &= [s_1(t) \quad s_2(t) \quad \cdots \quad s_P(t)]^T \end{aligned} \quad (4.4)$$

where P is the number of users, $\mathbf{n}(t)$ is the noise vector, and \mathbf{A} is defined as the *array manifold* whose columns are the spatial signatures.

For *broadband* signals where the delays between multipaths are not negligible, the memoryless spatial signature vector $\{\mathbf{a}_i\}$ must be replaced with vector FIR filters $\{\mathbf{h}_i(t)\}$, yielding the following input-output relation:

$$\mathbf{y}(t) = \sum_{i=1}^P \mathbf{h}_i(t) * s_i(t) + \mathbf{n}(t) \quad (4.5)$$

To utilize conventional spatial processing techniques developed for narrowband applications, one can apply OFDM to convert the broadband channel into N parallel narrowband subchannels:

$$\mathbf{y}(k, t) = \sum_{i=1}^P \mathbf{a}_{k,i} s_i(k, t) + \mathbf{n}(k, t), k = 1, \dots, N \quad (4.6)$$

where k is the subcarrier index, and $\mathbf{a}_{k,i}$ is the spatial signature of the i th user at subcarrier frequency k . As a result, parallel implementation of narrowband spatial processing algorithms becomes readily applicable on individual subcarriers.

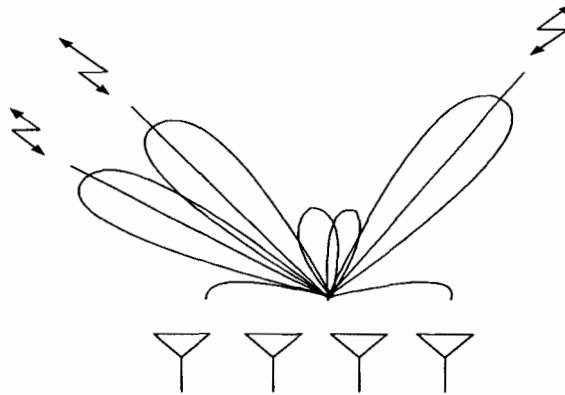


Figure 4.2: Antenna array and beamforming

4.2 Beamforming

Antenna array beamforming has been an active topic for wireless communications for the last 30 years. Beamforming is a linear space-time process that enhances the signal-of-interest through *weight-and-sum* operations. Beamforming can be performed both in transmission (TX) and reception (RX).

Consider the RX array output expressed in Equation (4.4). The signal-of-interest, say, $s_i(t)$, is subject to both interference and noise. A beamformer can extract $s_i(t)$ from $\mathbf{y}(t)$ by properly combining the M antenna outputs with a set of weights $\mathbf{w}_i = [w_{i,1}, w_{i,2}, \dots, w_{i,M}]^T$:

$$\begin{aligned}\hat{s}_i(t) &= \mathbf{w}^H \mathbf{y} = \sum_{m=1}^M w_{i,m}^* y_m(t) \\ &= \mathbf{w}_i^H \mathbf{a}_i s_i(t) + \sum_{j=1, j \neq i}^P \mathbf{w}_i^H \mathbf{a}_j s_j(t) + \mathbf{w}_i^H \mathbf{n}(t).\end{aligned}\quad (4.7)$$

A few representative beamformers are described here based on the way a weight vector is constructed.

4.2.1 Coherent combining

The coherent combiner is essentially a “single-user” beamformer in the sense that it performs beamforming solely based on \mathbf{a}_i without regard to the interference or noise characteristics.

$$\begin{aligned}\mathbf{w}_i &= \mathbf{a}_i \\ \hat{s}_i(t) &= \|\mathbf{a}_i\|^2 s_i(t) + \sum_{k=1, k \neq i}^K \mathbf{a}_i^H \mathbf{a}_k s_k(t) + \mathbf{a}_i^H \mathbf{n}(t).\end{aligned}$$

While enhancing the SINR of the signal-of-interest, the coherent combiner also suppresses interference since the spatial signatures are independent in general. The scheme is effective in the presence of a large number of interfering signals.

4.2.2 Zero-forcing

In the presence of a limited number of dominant interfering signals, a more effective scheme is the zero-forcing beamformer. Instead of suppressing the interference, a zero-forcing beamformer cancels out interference by putting a null in the direction defined by its spatial signature.

$$\begin{aligned}\mathbf{w}_i &: \mathbf{w}_i^H \mathbf{a}_j = \delta_{i,j} \\ \hat{s}_i(t) &= s_i(t) + \mathbf{w}_i^H \mathbf{n}(t)\end{aligned}$$

Given an array with M elements, the maximum number of interferences that can be eliminated is $M - 1$.

4.2.3 MMSE reception (optimum linear receiver)

The zero-forcing beamformer, while eliminating the interference, may at the same time amplify the noise due to its sidelobes. The “optimum” beamformer is defined as the one that minimizes the mean-squared error (MMSE) between the transmitted signal and the beamformer output:

$$\mathbf{w}_{i,mmse} = \arg_{\mathbf{w}_i} \min E\{\hat{s}_i(t) - s_i(t)\}$$

Using the orthogonality principle [2], one can easily obtain the MMSE beamformer as follows:

$$\begin{aligned}\mathbf{w}_{i,mmse} &= \mathbf{R}_y^{-1} \mathbf{a}_i \\ MSE_i &= 1 - \mathbf{a}_i^H \mathbf{R}_y^{-1} \mathbf{a}_i \\ SINR_i &= \frac{|\mathbf{a}_i^H \mathbf{R}_y^{-1} \mathbf{a}_i|^2}{|\sum_{j=1, j \neq i}^M \mathbf{a}_i^H \mathbf{R}_y^{-1} \mathbf{a}_j|^2 + |\mathbf{a}_i^H \mathbf{R}_y^{-1} \mathbf{a}_i|^2 \sigma_n^2}\end{aligned}$$

where $\mathbf{R}_y = E\{\mathbf{y}\mathbf{y}^H\}$ is the covariance matrix of the array output.

The most obvious benefit of beamforming is the SINR gain, as shown in the following propositions. Another key benefit is the increase in diversity order,

which is critical in fading channels. More discussion will be provided in later Sections.

Proposition 1 *For RX beamforming, the average SNR increases linearly with respect to the number of receivers.*

Proof. In RX beamforming,

$$\mathbf{y} = \mathbf{a}s + \mathbf{n}$$

where

$$\mathbf{n} \sim N(\mathbf{0}, \sigma_n^2 \mathbf{I}); \quad \text{var}(s) = \sigma_s^2$$

Applying the matched filter theorem, the optimum beamformer is given by

$$\begin{aligned} \mathbf{w} &= \alpha \mathbf{a} \\ \hat{s} &= \mathbf{w}^H \mathbf{y} \end{aligned} \tag{4.8}$$

Assuming that the channel elements $\{a_m\}$ are i.i.d. with variance σ_a^2 , and the resulting SNR is thus

$$SNR = \frac{\|\mathbf{a}\|^2}{\sigma_n^2} \sigma_s^2 \Rightarrow E\{SNR\} = M \frac{\sigma_s^2 \sigma_a^2}{\sigma_n^2}$$

■

It is important to realize that (i) the linear increase in SNR does not necessarily transfer into a linear data rate increase due to the diminishing return in achievable data rate; and (ii) RX beamforming also provides an increase in diversity order to M which is important in fading channels.

Transmit beamforming can be carried out in a similar fashion. Consider the case with M transmitters and 1 receiver, the TX beamformer weights the signal $s(t)$ with an $M \times 1$ vector before delivering them over the M transmitters:

$$\mathbf{x}(t) = \mathbf{w}s(t)$$

The receiver output is the superposition of the M copies of the original signal, attenuated by the channel coefficients:

$$y = \sum_{i=1}^M a_i^* x_i(t) = \mathbf{a}^H \mathbf{w} s(t) \tag{4.9}$$

The duality between receive beamforming (4.8) and transmit beamforming (4.9) is obvious.

Proposition 2 *For TX beamforming, the average SNR increases linearly with respect to the number of transmitters.*

Proof. In TX beamforming, the transmitted signal is

$$\mathbf{x} = \mathbf{ws}$$

whereas the received signal is a scalar

$$y = \mathbf{a}^H \mathbf{ws} + n \quad (4.10)$$

The optimum TX beamformer, subject to the total power constraint $\|\mathbf{w}\| = 1$, is

$$\mathbf{w} = \mathbf{a} / \|\mathbf{a}\|,$$

and the resulting SNR is given by

$$SNR = \frac{\|\mathbf{a}\|^2}{\sigma_n^2} \sigma_s^2 \Rightarrow E\{SNR\} = M \frac{\sigma_s^2 \sigma_a^2}{\sigma_n^2} \quad (4.11)$$

■

In many practical situations, the increase of transmit antennas also means a linear increase in total powers. In this case, the average SNR will increase quadratically with respect to the number of transmitters.

4.2.4 SDMA

Space-division multiple-access augments regular multiple-access schemes such as TDMA and CDMA by accommodating multiple users (signals) in one radio resource unit (time or frequency, or code). The idea is to multiplex signals spatially using beamforming or other more aggressive multiuser detection methods. Conceptually, SDMA can *multiply* the network capacity without additional radio resources. In reality however, the ability to separate co-channel signals depends critically on the spatial characteristics of the multiple users.

In RX SDMA, a commonly used multiuser detector is the beamformer. Using the result in (4.7), signal separation can be accomplished by

$$\hat{\mathbf{s}}(t) = \begin{bmatrix} \hat{s}_1(t) \\ \vdots \\ \hat{s}_P(t) \end{bmatrix} = \begin{bmatrix} \mathbf{w}_1^H \mathbf{y}(t) \\ \vdots \\ \mathbf{w}_P^H \mathbf{y}(t) \end{bmatrix} = \mathbf{W}^H \mathbf{y}(t).$$

The beamforming matrix \mathbf{W} can be constructed based on any of the aforementioned principles. Otherwise nonlinear detection, e.g., the maximum likelihood detection can be employed to recover the multiple symbol streams:

$$\hat{\mathbf{s}}(t) = \begin{bmatrix} \hat{s}_1(t) \\ \vdots \\ \hat{s}_P(t) \end{bmatrix}^T = \arg_{s_i(t) \in \mathcal{S}} \min \left\| \mathbf{y}(t) - \sum_{k=1}^P \mathbf{a}_k s_k(t) \right\|^2$$

where \mathcal{S} is the finite set of all possible symbol waveforms.

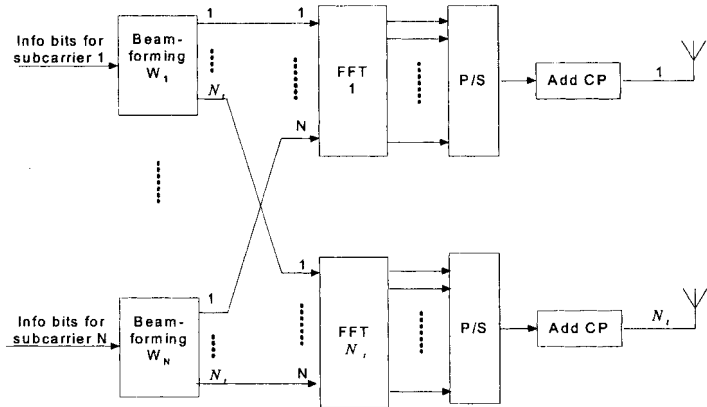


Figure 4.3: Broadband beamforming with OFDM

4.2.5 Broadband beamforming

If the signals are broadband as modeled in (4.5), the conventional narrowband beamforming techniques are not directly applicable.

Fortunately with OFDM, the broadband channel can be converted into parallel narrowband subchannels as in (4.6). Accordingly, narrowband beamforming can be implemented on individual subchannels. Figure 4.3 depicts the general block diagram of OFDM TX beamforming. The OFDM RX beamformers can be similarly constructed on subcarriers. Notice that since the broadband channels are *frequency selective*, the spatial channel characteristics vary from subcarrier to subcarrier. By default, different beamforming vectors will be needed on different subchannels. In practical situations, further channel structure information can be exploited to simplify the spatial operations - see ensuring sections for more discussions.

As a final note on beamforming, it must be pointed out that in practice the TX beamforming is significantly more challenging than RX beamforming for the following reasons:

- *Difficulty in obtaining the TX spatial signature*: the RX spatial signature in (4.3) and the TX spatial signature (4.10) are both time and frequency dependent, and therefore different in general. While the RX spatial signature, \mathbf{a}_R , can be estimated along with the received signals, the TX spatial signature, \mathbf{a}_T , can only be obtained indirectly. In a TDD (time-division multiplexing) system for example, one can estimate \mathbf{a}_T as $\mathbf{a}_T = \mathbf{a}_R$. However such an assumption is only valid if the TDD time frames are short

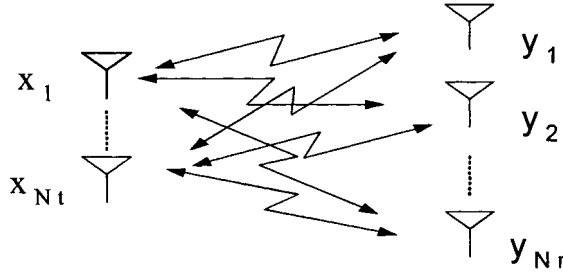


Figure 4.4: MIMO channel illustration

relative to the coherent time of the channels. This approach may be problematic in asymmetric data system where the availability of RX signals is not guaranteed.

- *Hardware induced phase ambiguity:* Both (4.3) and (4.10) ignore the fact that practical transceiver hardware is not perfectly balanced or aligned. In reality the *composite RX and TX* spatial signatures are given by

$$\begin{aligned}\mathbf{g}_R \odot \mathbf{a}_R &= [g_R(1)a_R(1) \quad g_R(2)a_R(2) \quad \cdots \quad g_R(M)a_R(M)]^T \\ \mathbf{g}_T \odot \mathbf{a}_T &= [g_T(1)a_T(1) \quad g_T(2)a_T(2) \quad \cdots \quad g_T(M)a_T(M)]^T\end{aligned}$$

respectively, where \mathbf{g}_R is the complex gain vector of the receiver hardware chains and \mathbf{g}_T is the complex gain vector of the transmit hardware chains. In most RX processing, only the composite spatial signature is needed. Such is not the case in TX beamforming where \mathbf{g}_R , or at least $\{g_T(m)/g_R(m)\}$, must be calibrated and compensated.

- *Broadband channels:* the calibration problem is further complicated by the fact that both $[\mathbf{a}_R, \mathbf{a}_T]$ and $[\mathbf{g}_R, \mathbf{g}_T]$ are frequency dependent in broadband systems.

4.3 MIMO channels and capacity

Traditional beamforming assumes multiple antennas at either the transmitter or the receiver side. When antenna arrays are available at both the transmitter and the receiver as shown in Figure 4.4, they create a channel function that has multiple-input and multiple-output (MIMO). The MIMO architecture has inspired much breakthrough research since 1996 [3]. In the following, we examine the potential of MIMO channels by evaluating its capacity.

From (4.3), a MIMO channel with N_t transmitters and N_r receivers can be written as follows, if the channel is flat:

$$\begin{bmatrix} y_1 \\ y_2 \\ \vdots \\ y_{N_r} \end{bmatrix} = \begin{bmatrix} h_{11} & h_{12} & \cdots & h_{1N_t} \\ h_{21} & h_{22} & \cdots & h_{2N_t} \\ \vdots & \vdots & \ddots & \vdots \\ h_{N_r 1} & h_{N_r 2} & \cdots & h_{N_r N_t} \end{bmatrix} \begin{bmatrix} x_1 \\ x_2 \\ \vdots \\ x_{N_t} \end{bmatrix}. \quad (4.12)$$

Using a more compact matrix representation,

$$\mathbf{y}_{N_r \times 1} = \mathbf{H}_{N_r \times N_t} \mathbf{x}_{N_t}.$$

In the above we replace s with the transmitted signal vector \mathbf{x} as the *space-time coded* version of the symbol sequence.

For broadband scenarios that involve L distinct multipath clusters,

$$\mathbf{y}(t) = \sum_{l=1}^L \mathbf{H}_l \mathbf{x}(t - \tau_l) \quad (4.13)$$

where each \mathbf{H}_l is an $N_r \times N_t$ matrix.

As will become clear in the following discussion, the *capacity* of the MIMO channel depends on the characteristics of the channel, both statistically and algebraically. While a common assumption of the channel is that \mathbf{H} is element-wise independent complex Gaussian random variables with zero mean, most practical channels do not fall under this category.

- Indoor micro MIMO: the ideal situation of MIMO involves rich scattering at both the transmitter side and the receiver side. In this case, it is reasonable to assume that each transmitter-receiver pair experiences independent fading and \mathbf{H} is complex Gaussian with $\mathbf{R}_{\mathbf{H}} = E \{ \mathbf{H} \mathbf{H}^H \} = \mathbf{I}$.
- Outdoor macro MIMO: Figure 4.5 illustrates an outdoor scenario where there are L multipaths from the base antenna array having distinct angles. Here the base-station is placed high above ground and is not surrounded by local scatters. In contrast, the user station is assumed to have uncorrelated fading at the antennas due to the fact that usually a large number of local scatters exists around the mobile antenna. Hence the outdoor downlink channel matrix has *uncorrelated rows and correlated columns*, whereas the uplink channel matrix has *uncorrelated columns and correlated rows*.
- Distributed MIMO: a few other systems can be modeled as MIMO channels. One example is the *relay network* where a source signal is delivered to destination(s) through multiple relay nodes [8]. Other examples include distributed sensor networks [9] and single-frequency broadcasting networks.

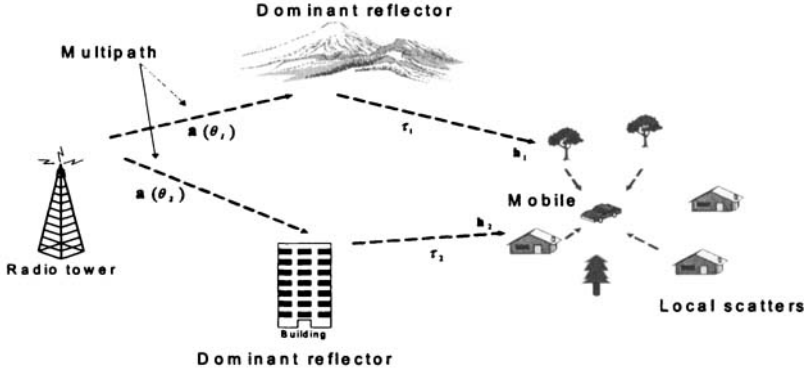


Figure 4.5: An outdoor wide-area MIMO scenario

A fundamental question in MIMO systems is its “capacity” with respect to the number of multiple transmitter antennas and receiver antennas. The answer can be found from an information theoretical viewpoint.

Given a MIMO channel, the mutual information between \mathbf{x} and \mathbf{y} is:

$$\begin{aligned}
 I(\mathbf{x}; \mathbf{y}) &= h(\mathbf{y}) - h(\mathbf{y}|\mathbf{x}) = h(\mathbf{y}) - h(\mathbf{n}) \\
 &= h(\mathbf{y}) - \sum_{i=1}^{N_r} h(n_i) \\
 &\leq \log((2\pi e)^{N_r} |\mathbf{R}_y|) - \sum_{i=1}^{N_r} h(n_i) \\
 &= \log((2\pi e)^{N_r} |\mathbf{R}_y|) - \frac{1}{2} \log((2\pi e)^{N_r} |\sigma^2 \mathbf{I}_{N_r}|) \\
 &= \log \frac{|\mathbf{R}_y|}{\sigma^2}
 \end{aligned}$$

where $\sigma^2 \mathbf{I}_{N_r} = E\{\mathbf{n}\mathbf{n}^H\}$, and $\mathbf{R}_y = E\{\mathbf{y}\mathbf{y}^H\} = \mathbf{H}\mathbf{R}_x\mathbf{H}^H + \sigma^2 \mathbf{I}_{N_r}$.

As a result, the MIMO capacity is given by

$$C = \log \left(\left| \mathbf{I} + \frac{\mathbf{H}\mathbf{R}_x\mathbf{H}^H}{\sigma^2} \right| \right) \quad (4.14)$$

If the channel characteristics \mathbf{H} are known to the transmitter (i.e., *informed*), it is possible to manipulate the transmit signal variance \mathbf{R}_x to maximize the channel capacity. On the other hand, if the channel information is not available

at the transmitter (i.e., *uninformed*), we let $\mathbf{R}_x = \frac{P}{N_t} \mathbf{I}_{N_t}$, i.e., equal power allocation over N_t transmitters with *fixed* total transmit power P . Then

$$C = \log \left(\left| \mathbf{I}_{\mathbf{R}} + \frac{P}{N_t} \frac{\mathbf{H}\mathbf{H}^H}{\sigma^2} \right| \right)$$

Denote $\rho = \frac{P}{\sigma^2}$ as the transmit signal to noise power ratio, then the capacity with parameter N_r and N_t per unit bandwidth is

$$C(N_t, N_r) = \log \left(\left| \mathbf{I} + \rho \frac{\mathbf{H}\mathbf{H}^H}{N_t} \right| \right). \quad (4.15)$$

- *SISO*: $\mathbf{H} = h$. With one transmit antenna and one receiver antenna, the channel capacity reduces to the classic result:

$$C(1, 1) = \log(1 + \rho|h|^2)$$

Observation: the capacity increases logarithmically with the SNR. Each extra bps/Hz requires roughly a doubling of the TX power. For example, to go from 1bps/Hz to 11bps/Hz, the TX power must be increased by roughly 1000 times!

- *MISO*: $\mathbf{H} = [h_1, h_2, \dots, h_{N_t}]$. This scenario is typically seen in cellular downlink with an antenna array at the base-station and a single antenna at the user terminal.

$$C(N_t, 1) = \log \left(1 + \rho \frac{|\mathbf{H}|^2}{N_t} \right) = \log \left(1 + \rho \frac{\sum_{i=1}^N |h_i|^2}{N_t} \right)$$

Observation: with the total transmission power fixed, the capacity actually does not increase with additional transmission antennas (unless \mathbf{H} is known at the transmitter, in which case transmit beamforming can be utilized to increase the SINR - see page 2). On the other hand, the *outage capacity* over a fading channel does improve due to the increased diversity.

- *SIMO*: $\mathbf{H} = [h_1, h_2, \dots, h_{N_r}]^T$. This scenario is typically seen in cellular uplink with an antenna array at the base-station and a single antenna at the user terminal.

$$C = \log \left(\left| \mathbf{I} + \rho \mathbf{H}\mathbf{H}^H \right| \right).$$

Since $|\mathbf{I}_{N_r} + \rho \mathbf{H}\mathbf{H}^H| = |\mathbf{I}_{N_t} + \rho \mathbf{H}^H \mathbf{H}|$, we get

$$C = \log \left(1 + \rho |\mathbf{H}|^2 \right) = \log \left(1 + \rho \sum_{i=1}^{N_r} |h_i|^2 \right).$$

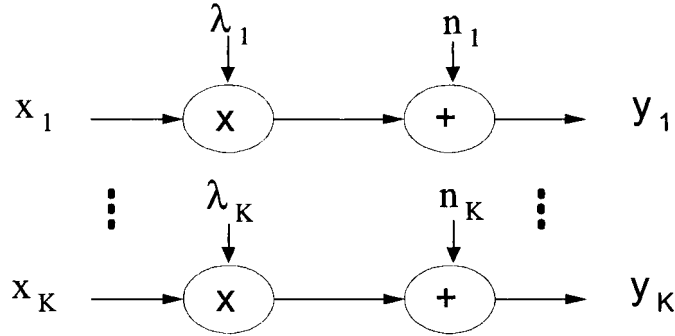


Figure 4.6: An equivalent parallel SISO representation of the MIMO channel.

Observation: the capacity increases logarithmically with respect to the number of antennas at the receiver side.

- *MIMO:* To gain insight to the MIMO scenario, let us perform an eigenvalue decomposition on the channel matrix as following

$$\mathbf{H}\mathbf{H}^H = \mathbf{E}\Lambda\mathbf{E}^H.$$

We obtain from (4.15)

$$C = \sum_{k=1}^K \log \left(\left| 1 + \rho \frac{\lambda_k}{N} \right| \right).$$

where $\{\lambda_k\}$ are the K non-zero eigenvalues of the channel covariance. It is seen that the MIMO channel can be decomposed into K multiple parallel SISO channels that can be used to deliver information simultaneously, indicating the potentially linear increase in capacity with respect to $K \leq \min(N_r, N_t)$. An equivalent representation of the MIMO channel is given in Figure 4.6.

Note that the distribution of $\{\lambda_k\}$ is determined by the condition of the channel matrix. It can be shown that the maximum capacity is achieved when $\lambda_1 = \lambda_2 = \dots = \lambda_k$, in which case

$$C = K \log \left(\left| 1 + \frac{\rho}{N} \right| \right).$$

- Broadband MIMO: from (4.13), the channel response in frequency domain is given by.

$$\mathbf{H}(\omega) = \sum_{l=1}^L \mathbf{H}_l e^{-j\omega l}$$

The total capacity is obtained by replacing \mathbf{H} in (4.14) with $\mathbf{H}(\omega)$, and integrating over the frequency band [7].

4.4 Space-time coding

To capture the potential of MIMO channels promised by (4.14) and (4.15), multiple-antenna transmission schemes as well as sophisticated MIMO receiver techniques need to be developed. In this section, we discuss the basic principles of space-time coding and lay some groundwork for Section 4.5.

In the most generic form, a space-time encoder provides a mapping between the information-bearing symbols $\{s\}$ to an N_t -dimensional stream \mathbf{c} ($\mathbf{x} = \mathbf{c}$ if no additional operation is involved)

$$\{s\} \implies \{\mathbf{c}\}$$

Each element of \mathbf{x} is transmitted simultaneously from a different transmit antenna as specified in (4.12). We define the space-time coding rate R_{ST} as

$$R_{ST} = \text{the number of symbols/transmission}$$

The actual data rate (bit/second) depends on how many bits each symbol carries.

4.4.1 Spatial multiplexing

The spatial multiplexing scheme sends independent data streams over the individual TX channels. The best known example is the Bell Labs Layered Space-time Architecture (BLAST) which has the following mapping [3]:

$$\mathbf{c}(k) = \mathbf{x}(k) = \begin{bmatrix} s(N_t k + 1) \\ s(N_t k + 2) \\ \vdots \\ s(N_t k + N_t) \end{bmatrix}.$$

As a result, spatial multiplexing offers the maximum rate of $R_{ST} = N_t$. If $N_r \geq N_t$, the symbol streams can be recovered by inverting the MIMO channel:

$$\hat{\mathbf{s}} = \mathbf{H}^\dagger \mathbf{y}$$

Spatial multiplexing is rather simple and has good behavior in environment with high scattering. The data rate can be extremely high in favorable channel conditions (high SNR and high scattering). On the other hand, its performance decreases with increasing spatial correlation in the channel. In addition, on the receiver side we need at least as many antennas as on the transmitter side

4.4.2 Orthogonal space-time block coding

Alamouti [4] discovered a remarkable space-time block coding scheme that achieves both SINR gain and diversity gain with two transmit antennas. The scheme was later generalized into a class of *orthogonal space-time block* codes (OSTBC) that promises full transmit diversity and simple reception [11].

The Alamouti code is a rate-1($R_{ST} = 1$) orthogonal space-time block code with the following mapping

$$\mathbf{s} = \begin{bmatrix} s_1 \\ s_2 \end{bmatrix} \implies \mathbf{X} = [\mathbf{x}(1) \quad \mathbf{x}(2)] = \begin{bmatrix} s_1 & -s_2^* \\ s_2 & s_1^* \end{bmatrix}$$

The two symbols are transmitted over two time units from the two antennas. At the receiver side, the received signal over two consecutive symbols are

$$\begin{aligned} y(1) &= h_1 s_1 + h_2 s_2 + n_1 \\ y(2) &= -h_1 s_2^* + h_2 s_1^* + n_2 \end{aligned}$$

By stacking the two consecutive received signals as

$$\mathbf{r} = [y(1) \quad y^*(2)]^T$$

we have

$$\mathbf{r} = \mathbf{Gs} + \mathbf{n}; \quad \mathbf{G} = \begin{bmatrix} h_1 & h_2 \\ h_2^* & -h_1^* \end{bmatrix}$$

where $\mathbf{n} = [n_1 \quad n_2]^T$.

The maximum likelihood decoder is given by

$$\hat{\mathbf{s}} = \arg \min_{\hat{\mathbf{s}} \in \mathcal{C}} \|\mathbf{r} - \mathbf{G}\hat{\mathbf{s}}\|^2$$

Notice that the \mathbf{G} matrix is orthogonal, i.e., $\mathbf{G}^H \mathbf{G} = \rho \mathbf{I}$, where $\rho = |h_1|^2 + |h_2|^2$. We may modify the signal vector and reduce the ML decoding to:

$$\begin{aligned} \hat{\mathbf{r}} &= \mathbf{G}^H \mathbf{r} = \rho \mathbf{s} + \hat{\mathbf{n}} \\ \hat{\mathbf{s}} &= \arg \min_{\mathbf{s} \in \mathcal{S}} \|\hat{\mathbf{r}} - \rho \mathbf{s}\|^2 \end{aligned}$$

Surprisingly, the decoding rule in the above ML formulation reduces to two independent, much simpler decoding rules for s_1 and s_2 . Because the symbols are transmitted from two antennas, it is easy to verify that an order-2 transmit diversity is achievable. On the other hand, since no channel information is

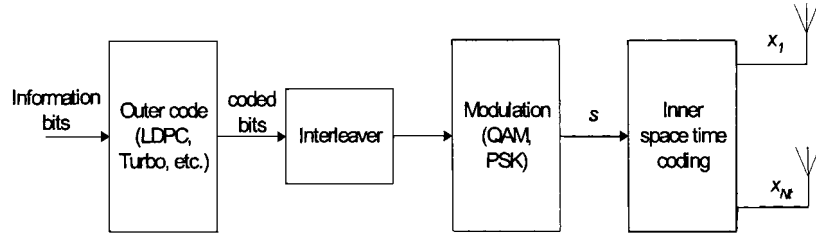


Figure 4.7: An MIMO system block diagram

utilized at the transmit, the SINR gain of Alamouti code should not be as significant as downlink beamforming (4.11). Such is indeed the case as the SNR of the decoder output is given by

$$SNR = \frac{(|h_1|^2 + |h_2|^2)}{\sigma_n^2} \frac{\sigma_s^2}{2} \Rightarrow E\{SNR\} = \frac{\sigma_s^2 \sigma_a^2}{\sigma_n^2} \quad (4.16)$$

A factor of 2 is introduced in the SNR calculation to normalize the total transmitted power to σ_s^2 . Compared to (4.11), it is obvious that the Alamouti scheme is at a 3dB SNR disadvantage to the beamforming scheme.

Orthogonal space-time block codes for $N_t > 2$ are available, but only for $R_{ST} < 1$ symbols/transmission [11]. In addition, the OSTC does not introduce any coding gain. Non-orthogonal space-time block codes based on linear complex field enable full diversity without any rate loss (1 symbol/transmission)

4.4.3 Concatenated ST transmitter

For actual systems, STC is used in combination with an outer channel encoder as depicted in Figure 4.7. Essentially, it forms a serial concatenation of turbo encoder where an iterative detection and decoding strategy can be employed at the receiver side [6].

- The channel encoder, e.g., the LDPC or convolutional encoders, provides an outer code that can be decoded by a soft-input soft-output decoder.
- The interleaver interleaves the coded bit stream on a block-by-block basis. The output stream is mapped onto QAM or M-ary PSK symbols.
- A linear space-time encoder provides the tradeoff between the data rate and diversity order, with extreme cases being the BLAST (highest rate) and the OSTBC (full diversity).

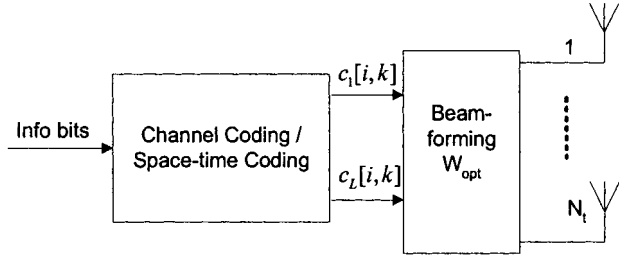


Figure 4.8: Beamforming with ST coding

A wide variety of decoding schemes can be used, offering tradeoffs between performance and complexity [6]. The overall rate of the transmitter is determined by

$$R_{TX} = R_{\text{outer code}} \times R_{\text{QAM}} [\text{bits/symbol}] \times R_{ST} [\text{symbol/s}].$$

Determining the optimum combination for a given channel involves at least three parameters: the outer channel coding rate, the modulation scheme, and the STC rate. The tradeoffs between the three sub-modules in a space-time transmitter remain to be fully investigated.

4.4.4 Beamforming with ST coding

In some applications where MIMO channel information is known at the transmission side (even partially), transmit beamforming in addition to the space-time coding can be employed to further improve the system performance. A block diagram of the combination of space-time coding with transmit beamforming is illustrated in Figure 4.8. Transmit beamforming utilizes certain knowledge of the channel to achieve transmit antenna array gains. The optimal transmitter design has previously been investigated in [12][13] based on a capacity criterion. To understand the potential, let us investigate the change of capacity if the transmitter is informed.

From (4.14), we can see that by letting

$$\{s\} \implies \{\mathbf{c}\} \implies \mathbf{x} = \mathbf{W}\mathbf{c}$$

where \mathbf{c} is the space-time coded vector which is assumed to be i.i.d. statistically. One can change the covariance matrix of \mathbf{x} by adjusting the beamforming matrix \mathbf{W} . If the channel matrix \mathbf{H} is fully known at the transmitter, the optimum beamformer that maximizes the channel capacity is then found to be

$$\begin{aligned}\mathbf{W}_{opt} &= \arg_{\mathbf{W}} \max \left| \mathbf{I}_R + \frac{\mathbf{H} \mathbf{W} \mathbf{W}^H \mathbf{H}^H}{\sigma^2} \right| \\ \text{subject to} &\quad \text{tr}[\mathbf{W} \mathbf{W}^H] = 1\end{aligned}$$

In many applications, full knowledge of the channel is often not available. Rather, the statistical information of the channel may be estimated. For example, we can assume that the channel can be expressed as

$$\mathbf{H} = \mathbf{H}_r \mathbf{R}_H^{1/2} \quad (4.17)$$

where \mathbf{H}_r is i.i.d complex Gaussian, and \mathbf{R}_H is the transmit antenna correlation matrix. In this case, statistical beamforming in conjunction with space-time coding can be applied. Sampath and Paulraj [5] and Zhou and Giannakis introduced the notion of eigen-beamforming using orthogonal space-time block codes and vector channel covariance matrices [14]. Focusing on symbol-by-symbol detection, the optimal beamforming was designed in [16] to minimize symbol error rate (SER).

Consider a size $L \times K$ space-time block code

$$\mathbf{C} = [\mathbf{c}(1) \quad \mathbf{c}(2) \quad \dots \quad \mathbf{c}(K)].$$

Instead of transmitting \mathbf{C} directly through N_t antennas, an $N_t \times L$ beamforming transmit beamforming matrix \mathbf{W} is applied, given the following transmitted signal

$$\mathbf{X} = \mathbf{WC}$$

Then the received signal becomes

$$\mathbf{Y} = \mathbf{HX} = \mathbf{HWC}$$

The optimum *statistical* beamformer is the one that optimizes the error performance. Based on pairwise error probability of the receiver with ML detection established in [10], it is straightforward to show that the probability of the decoder deciding in favor of code word \mathbf{C}^e , when in fact the code matrix \mathbf{C} was transmitted, is upper bounded as

$$P_e \leq P(\mathbf{C} \rightarrow \mathbf{C}^e) \leq \exp(-\|\mathbf{H} \mathbf{W}(\mathbf{C} - \mathbf{C}^e)\|_F^2 / 4N_o) \quad (4.18)$$

Averaging across all possible channel realizations, the average PEP is shown as

$$\bar{P}_e = E_{\mathbf{H}}\{P_e\} \leq c \left| \mathbf{I} + \frac{(\mathbf{C} - \mathbf{C}^e)(\mathbf{C} - \mathbf{C}^e)^H \mathbf{W}^H \mathbf{R}_H \mathbf{W}}{4N_o} \right|^{-N_r}$$

from which the optimum beamformer \mathbf{W}_{opt} can be derived.

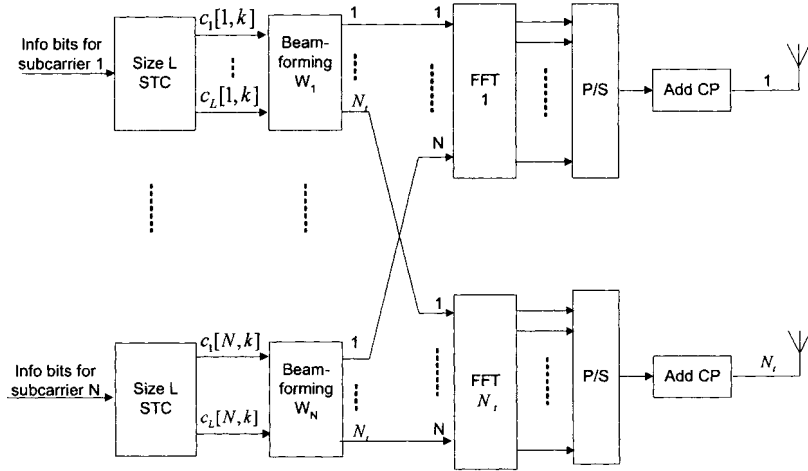


Figure 4.9: STC with beamforming in OFDM

4.4.5 ST beamforming in OFDM

The ST beamforming principles can be applied to broadband system using OFDM modem. By transforming the broadband channels into a set of parallel narrowband subchannels, the space-time coding beamforming can take the canonical form depicted in Figure 4.9.

4.5 Wide-area MIMO beamforming

Much of the work to date on STC-OFDM assumes a multipath channel in which fading from each transmit antenna to any receive antenna is independent. Such is valid only in a rich scattering environment. In many wide-area applications, the base station (BTS) is usually placed high above the ground and is not surrounded by scatters. The multipaths at the basestation antenna array will have distinct angles with each multipath corresponding to a distant scatter. As a result, the fadings in the MIMO channel are correlated with each other. Since the BTS-to-user transmission is more important in asymmetric applications, there is a strong need for an optimized space-time downlink modem for such channel conditions. In this section, we present a downlink MIMO beamforming scheme suitable for outdoor applications.

4.5.1 Data model

Negi *et al.* introduced a downlink beamforming STC scheme specifically for outdoor channels [15]. Here, we describe a low-complexity transmission scheme for

broadband OFDM operations. The approach offers the benefits of both transmit beamforming and space-time coding to an OFDM system without minimum increase in complexity. In the outdoor channel model, the optimum beamformer is shown to be identical for all subcarriers in the OFDM system, allowing simple time domain implementation of the transmit beamformer and a simpler receiver.

Referring to Figure 4.5 which depicts the downlink scenario under consideration, the $N_r \times 1$ received signal at the mobile station can be expressed as [15]

$$\mathbf{y}(k) = \sum_{l=1}^L \mathbf{h}_l \mathbf{a}^H(\theta_l) \mathbf{x}(k - \tau_l) + \mathbf{v}(k)$$

where k denotes the discrete time index and τ_l is the discrete delay for path l ; $\mathbf{h}_l = [h_{l1} \cdots h_{lN_r}]^T$ is the $N_r \times 1$ vector of fading channel gains associated with the l th multipath; $\mathbf{a}(\theta_l)$ is the $N_t \times 1$ vector representing the array response for the l th path at angle θ_l ; $\mathbf{x}(k) = [x_1(k) \cdots x_{N_t}(k)]^T$ is the $N_t \times 1$ vector of the transmitted signal, and $\mathbf{v}(k)$ is the $N_r \times 1$ noise vector at the receive antennas.

In the above model, the fading gain vectors $\{\mathbf{h}_l\}$ for the L distinct paths are assumed to be uncorrelated. Also, their elements are assumed to have independent and identically distributed Rayleigh fading due to the abundant local scatters around the mobile. Each $\mathbf{h}_l \mathbf{a}^H(\theta_l)$ forms an $N_r \times N_t$ MIMO matrix \mathbf{H} , whose columns are correlated. We further assume that

- the BTS has knowledge of the multipath angles $\{\theta_l\}$ which are slow changing in an outdoor environment;
- the BTS does not know the fading gains \mathbf{h}_l since they may be fast varying due to the motion of the terminal and environment variations;
- the mobile has full knowledge of channel state information (CSI) through channel estimation.

With an N -subcarrier OFDM, the input-output relation for the i th subcarrier in this system can be expressed as

$$\mathbf{y}(i, k) = \sum_{l=1}^L [\mathbf{h}_l \mathbf{a}^H(\theta_l) e^{-j \frac{2\pi}{N} \tau_l i}] \mathbf{x}(i, k) + \mathbf{v}(i, k), i = 1, \dots, N$$

Written in matrix form, we have

$$\mathbf{y}(i, k) = \mathbf{H} \mathbf{D}_i \mathbf{A}^H \mathbf{x}(i, k) + \mathbf{v}(i, k)$$

where $\mathbf{H} = [\mathbf{h}_1 \cdots \mathbf{h}_L]$, $\mathbf{A} = [\mathbf{a}(\theta_1) \cdots \mathbf{a}(\theta_L)]$, and

$$\mathbf{D}_i = \text{diag} \left\{ e^{-j \frac{2\pi}{N} \tau_1 i}, \dots, e^{-j \frac{2\pi}{N} \tau_L i} \right\}.$$

For conventional STC-OFDM transmission over uncorrelated broadband MIMO channels, a size N_t space-time code is needed on each subcarrier to achieve the full spatial diversity. However in our channel model there are only L independent paths, the total order of diversity available from the channel is $N_r L$ instead of $N_r N_t L$, suggesting a STC of size L is sufficient [15]. Without utilizing the channel structure or the angle information, the conventional STC scheme is sub-optimum in terms of both performance (i.e., no beamforming gain) and complexity (oversized STCs and FFT operations). In the following, we will develop a scheme to achieve better performance at lower complexity.

4.5.2 Uncoded OFDM design criterion

Since the maximum diversity in the system is $N_r L$, we start with a size L space time code which is able to capture L -order diversity in uncorrelated MIMO channels. Now for each subcarrier, we employ a size $L \times K$ space-time code $\mathbf{C}_i = [\mathbf{c}_i(1) \ \mathbf{c}_i(2) \ \cdots \ \mathbf{c}_i(K)]$. Combined with a transmit beamforming matrix \mathbf{W}_i , the transmitted signal on the i th subcarrier is

$$\mathbf{X}_i = \mathbf{W}_i \mathbf{C}_i$$

where \mathbf{X}_i is the transmitted symbol on the i th subcarrier over K OFDM symbols. Then the received signal at subcarrier i is

$$\mathbf{Y}_i = \mathbf{H} \mathbf{D}_i \mathbf{A}^H \mathbf{W}_i \mathbf{C}_i + \mathbf{V}_i$$

where $\mathbf{Y}_i = [\mathbf{y}_i(1) \ \mathbf{y}_i(2) \ \cdots \ \mathbf{y}_i(K)]$. To find the best transmission scheme in terms of error performance, let us first derive the performance criteria of the above STC coded system. From (4.18), the probability of the decoder deciding in favor of code word \mathbf{C}_i^e , when in fact the code matrix \mathbf{C}_i was transmitted, is upper bounded as

$$P_e \leq P(\mathbf{C} \rightarrow \mathbf{C}^e) \leq \exp(-|\mathbf{H} \mathbf{D}_i \mathbf{A}^H \mathbf{W}_i (\mathbf{C} - \mathbf{C}^e)|_F^2 / 4N_o) \quad (4.19)$$

Averaging across all possible channel realizations, the average PEP is shown in Appendix I as

$$\overline{P}_e = \left(\frac{1}{4N_o} \right)^{-N_r L} \left| \mathbf{D}_i \mathbf{A}^H \mathbf{W}_i (\mathbf{C} - \mathbf{C}^e) (\mathbf{C} - \mathbf{C}^e)^H \mathbf{W}_i^H \mathbf{A} \mathbf{D}_i^H \right|^{-N_r} \quad (4.20)$$

Now we optimize \mathbf{W}_i for each subcarrier to minimize error probability. Since our objective is to design the optimum beamforming matrix for any pre-chosen space time codes \mathbf{C} , we can assume $|(\mathbf{C} - \mathbf{C}^e)(\mathbf{C} - \mathbf{C}^e)^H|$ to be a constant which does not affect the optimization result. With this assumption, the optimization problem reduces to

$$\begin{aligned} \min & \quad \left| \mathbf{D}_i \mathbf{A}^H \mathbf{W}_i \mathbf{W}_i^H \mathbf{A} \mathbf{D}_i^H \right| \\ \text{subject to} & \quad \text{tr}[\mathbf{W}_i \mathbf{W}_i^H] = L \end{aligned}$$

The constraint arises due to the total transmitted power over N_t antennas. Under unit transmit power assumption, a size L space-time code allocates an average power of $1/L$ to each of its L output symbols, i.e.,

$$E \{ \mathbf{c}(k) \mathbf{c}^H(k) \} = \mathbf{I}/L$$

The optimum solution is given by the following proposition.

Proposition 3 *The optimum beamforming matrix \mathbf{W}_{opt} for each subcarrier is identical, and is composed of the first L right singular vectors of matrix \mathbf{A}^H .*

Proof. Notice that matrix \mathbf{D}_i is orthogonal; the maximization criterion can be simplified as

$$\min \left| \mathbf{D}_i \mathbf{A}^H \mathbf{W}_i \mathbf{W}_i^H \mathbf{A} \mathbf{D}_i^H \right| = \min \left| \mathbf{A}^H \mathbf{W}_i \mathbf{W}_i^H \mathbf{A} \mathbf{D}_i^H \mathbf{D}_i \right| = \min | \mathbf{A}^H \mathbf{W}_i \mathbf{W}_i^H \mathbf{A} |$$

It is obvious that the optimum solution is only decided by the matrix \mathbf{A} and is independent of subcarrier index i . Following the similar derivation as in [15], we can show the optimum solution is to choose $\mathbf{W} = \mathbf{Q}_+ \Phi$, where Φ is an arbitrary orthogonal matrix, and \mathbf{Q}_+ is comprised of the first L right eigenvectors of matrix \mathbf{A}^H . A natural choice is to let Φ be an identity matrix, which leads to $\mathbf{W} = \mathbf{Q}_+$. ■

Due to the fact that beamforming vectors are identical for all subcarriers, the computation complexity for finding the beamforming matrix is dramatically reduced. In fact, beamforming can be performed in the time domain in an OFDM system, which can further reduce the transmitter complexity.

Proposition 4 *The outdoor STC-beamforming scheme can be realized with L IFFT operations, following by a size $L \times N_t$ beamformer as shown in Figure 4.10.*

Fig. 4.10 illustrates the TX structure of a STC-beamforming OFDM system. Note when the number of antennas N_t is greater than the number of path L , this transmission scheme can reduce the transmitter complexity, requiring only L FFT computations instead of N_t FFTs as in the conventional STC-OFDM system.

With the optimum beamforming transmission scheme, the effective channel at the receiver for the i th subcarrier in an OFDM system becomes the standard uncorrelated MIMO channel,

$$\mathbf{Y}_i = \mathbf{H}_{i,eff} \mathbf{C}_i + \mathbf{V}_i \quad (4.21)$$

$$\mathbf{H}_{i,eff} = [\sigma_1 \mathbf{h}'_1 \cdots \sigma_L \mathbf{h}'_L] \quad (4.22)$$

where σ_l are the L singular values of the matrix \mathbf{A}^H , and $[\sigma_1 \mathbf{h}'_1 \cdots \sigma_L \mathbf{h}'_L] = \mathbf{H} \mathbf{D}_i \mathbf{U}$, where \mathbf{U} is the left singular vectors of \mathbf{A}^H . Since both \mathbf{D}_i and \mathbf{U}

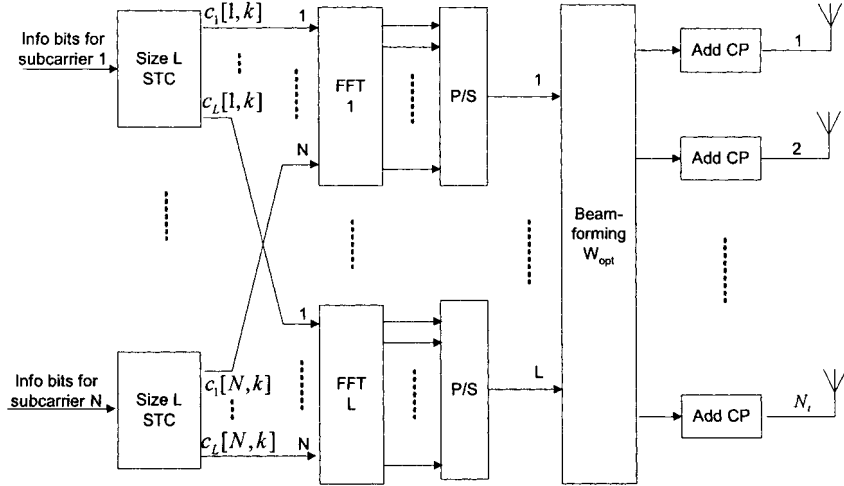


Figure 4.10: A simplified STC with beamforming architecture

are orthogonal matrices and \mathbf{H} has i.i.d complex Gaussian elements, $\{\mathbf{h}'_i\}$ are uncorrelated Rayleigh fading random vectors. Therefore, it is straightforward to show that with an L -diversity space-time code, a diversity order of N_rL is achieved.

To perform coherent detection, the receiver needs to estimate each subcarrier's effective channel $\mathbf{H}_{i,eff}$. With estimated channel coefficients, standard ML decoding can be employed to detect \mathbf{C}_i from \mathbf{Y}_i optimally,

$$\hat{\mathbf{C}}_i = \arg \min_{\mathbf{C}_i} |\mathbf{Y}_i - \mathbf{H}_{i,eff} \mathbf{C}_i|.$$

Note the complexity of ML decoding is exponentially proportional to the size of the STC, which is the number of available paths L . When L is less than the available antennas N_t at the basestation, a reduction in decoding complexity compared to the conventional STC-OFDM of the order of $N_t - L$ is achieved.

In addition to lower encoder and decoder complexity as explained above, the outdoor STC-beamforming scheme also has better error performance than the conventional STC-only scheme. Since the two schemes use different size space-time codes, it is difficult to compare the performance in terms of pairwise error probability in (4.20), which depends on the specific space-time code design. Instead, we use the average receiving SNR as a metric to compare the two schemes. The following proposition states that the STC-beamforming scheme enjoys an SNR gain of $10 \log \left(\frac{N_t}{L} \right)$ dB.

Proposition 5 *For a system with N_t transmit antennas and L distinct paths ($N_t > L$), the proposed STC-beamforming scheme has a receiving SNR gain of $10 \log \left(\frac{N_t}{L} \right) dB$ compared with the standard STC only scheme.*

Proof. See Appendix II. ■

4.5.3 Coded OFDM design criterion

In the previous section, we have demonstrated that combining beamforming with space-time codes can provide full diversity, achieve an SNR increase, and at the same time reduce the transmitter and receiver complexity. As mentioned in Section 4.4.3, an outer channel code is often employed in practical systems to combat frequency selectivity. A natural question here is how the outer channel encoder affects the ST-beamforming design in the outdoor ST-beamforming scheme.

Figure 4.11 shows the coded OFDM system under consideration. The information bits are first encoded with an outer channel code. We assume that the coding block spans more than one OFDM symbol and that the coded bits are fully interleaved before they are mapped to constellation points. A size \hat{L} space time code is employed on each subcarrier followed by standard OFDM modulation. As shown previously, beamforming can be performed in the time domain, which reduces the number of FFT operations to \hat{L} . In this section, we investigate the choice of \hat{L} and the beamformer \mathbf{W} in the presence of an outer channel encoder.

Paths with distinct delay

We first consider the case when all multipaths have distinct delays. The following proposition states that with a strong outer channel coding, all available diversity can be captured without a space-time code.

Proposition 6 *In a coded OFDM system, full diversity can be achieved by coding across subcarriers when all multipaths have distinct delays. Consequently no space-time code is needed and the beamforming vector should be chosen as the first right singular vector of the matrix \mathbf{A}^H .*

Proof. See Appendix III. ■

Intuitively, the above result can be understood from the fact that the composite channels across subcarriers contain different linear combinations of uncorrelated paths. Consequently, the outer channel code can capture all angle diversity in the frequency domain. At the same time, by transmitting all energy along the first right singular vector, the highest SNR gain is attained.

Paths with same delay

Proposition 6 shows that when all paths in the outdoor model have different arrival time, full diversity can be captured by using an outer code across subcarriers. In other words, the angle diversity is readily transferred into the frequency diversity in the OFDM systems. Combined with a proper beamformer, the transmission scheme can achieve both diversity and SNR gain as well. However, such a scheme can not fully exploit the available diversity in the channel when several paths have the same delay. This loss of diversity can be shown by observing (4.21). Notice that when two paths, say \mathbf{h}_1 and \mathbf{h}_2 , have the same delay τ_1 and τ_2 , these two coherent paths will always be combined in the same way on all subcarriers. Therefore, the available diversity in the effective channel seen by the channel coding is reduced. To capture this otherwise lost diversity, a space-time code is needed. The size of the STC needed is dependent on the number of paths having the same delay, as shown in the following proposition.

Proposition 7 *In a coded OFDM system, a size \hat{L} STC is needed to capture the \hat{L} order spatial diversity when \hat{L} paths have same delays. Combined with outer channel coding across subcarriers and beamforming with the first \hat{L} right singular vectors, the transmission scheme is able to achieve full diversity and the largest SNR gain.*

Proof. Suppose \hat{L} paths have the same delay τ_1 . Substituting the $N_t \times \hat{L}$ beamformer matrix \mathbf{W} into the channel model, we have the effective $N_t \times \hat{L}$ channel matrix for the i th subcarrier as

$$\mathbf{H}_{i,eff} = [\hat{\mathbf{h}}_{i,1} \cdots \hat{\mathbf{h}}_{i,\hat{L}}] = [\mathbf{h}_{i,1} \cdots \mathbf{h}_{i,L}] \mathbf{D}_i [\sigma_1 \mathbf{u}_1 \cdots \sigma_{\hat{L}} \mathbf{u}_{\hat{L}}]$$

It is easy to show that the \hat{L} columns of the effective channel matrix $\mathbf{H}_{i,eff}$ are uncorrelated by verifying that $E\{\hat{\mathbf{h}}_{i,j_1} \hat{\mathbf{h}}_{i,j_2}^H\} = 0$, for $j_1 \neq j_2$. Therefore a diversity order of \hat{L} is obtained with a conventional size \hat{L} space-time code [10]. The remaining diversity from paths with distinct delays can be obtained by outer channel coding across subcarriers, as demonstrated in Proposition 6. ■

Example 9 Consider a 256-point OFDM system with a uniform linear array with $N_t = 4$ antennas at the transmitter. Figure 4.12 compares the performance of the STC-beamforming scheme, the conventional STC (STC-only), and the beamforming-only scheme. The number of paths $L = 2$. The angles of departure (AOD) and the delays of these two paths are $\{10^\circ, 30^\circ\}$ and $\{1, 10\}$ (samples), respectively. The space-time code employed is the orthogonal space-time block code. For the STC-beamforming scheme, a size-2 orthogonal STBC, i.e., Alamouti code, is combined with beamforming as described. For the beamforming only

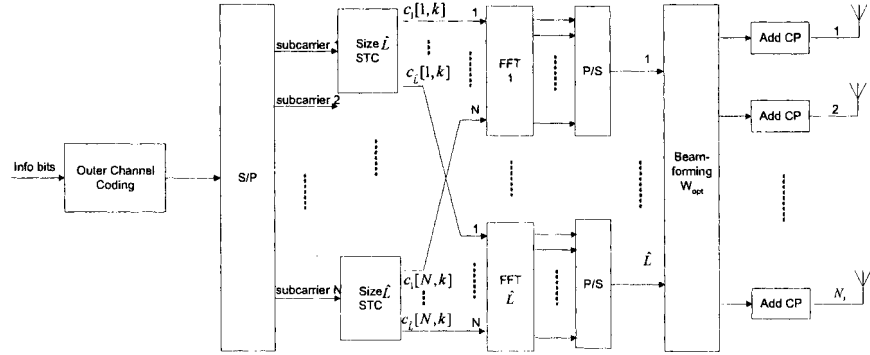


Figure 4.11: Concatenated coding in OFDM with beamforming

scheme, the beamformer vector is chosen as the first right singular vector, i.e. the dominant eigen-mode transmission. For the conventional STC transmission, a size-4 orthogonal STBC [11] with a rate of 1/2 is combined with 16QAM modulation to provide a spectral efficiency of 2 bits/symbol. The other two schemes use QPSK. This figure clearly shows that the STC-beamforming scheme has the best performance among all three. It has the same diversity order as the conventional STC scheme, while enjoying a SNR gain of about 5 dB. The larger SNR gain is partly due to the higher order modulation scheme used in the STC only scheme. Compared with the beamforming only scheme, the STC-beamforming scheme achieves a higher order of diversity as indicated by a steeper BER curve. It is also interesting to notice that BER curves for the conventional STC scheme and the beamforming only scheme cross over at $SNR = 19dB$. This is understandable since in the low SNR range, the beamforming-only scheme has better BER performance due to its SNR gain; while in the high SNR range, diversity becomes more important to performance. Although the size-4 STTC has a larger coding gain and a much higher decoding complexity, it is still outperformed by the 2-STTC combined with beamforming scheme. The SNR gain obtained by the STC-beamforming scheme is about 3dB, which is consistent with Proposition 5.

Example 10 Performance of STC-beamforming transmission in coded OFDM systems are evaluated in Fig. 4.13(a) and (b). A 1/2 rate 64-state convolutional code is used to encode information bits across 256 subcarriers. Fig. 4.13(a) compares the performance of the STC-beamforming and the beamforming-only schemes for the case where the two paths in the channel have distinct delays $\tau_1 = 1$ and $\tau_1 = 10$. The space-time code used is the Alamouti code. As expected, the two schemes have the same diversity order while the STC-beamforming scheme slightly outperforms the other scheme by about 1dB. The reason for this gain is that the space-time code produces a flatter channel across all subcarriers, which

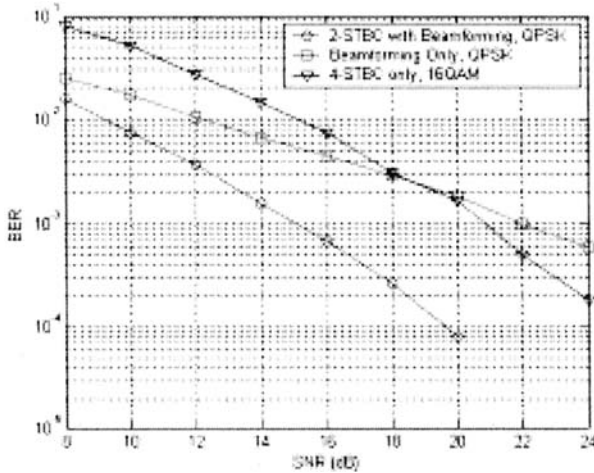


Figure 4.12: Performance of STC with beamforming vs. STC only schemes.

is more beneficial to the outer channel coding. Also plotted in the figure are the BER curves of the two schemes when there are $L = 4$ paths. Both schemes are able to pick up the higher order of diversity in this setup and provide similar performance. When several paths in the channel have same delays, the space-time code is needed to obtain all the diversity inherent to the channel. This effect is clearly demonstrated in the Fig. 4.13(b), where two channel setups are considered. For the first setup, there are 2 paths with the same propagation delay $\tau_1 = 1$. The number of antennas at the basestation is set to be 4. It is obvious that the beamforming only scheme can not achieve the diversity order of 2, even with the help of the FEC. Hence, it suffers a large performance loss in the high-SNR region. For the second channel setup, the number of distinct paths in the physical channel is assumed to be 4. The delays for these 4 paths are $\{1, 1, 10, 10\}$ respectively. Once again, it is seen that the Alamouti code combined with beamforming obtains the full diversity, while the beamforming-only scheme can only provide diversity of order 2. This is because the outer channel code across subcarriers can only exploit the diversity associated with paths having distinct delays, which in this case is 2.

4.6 Summary

Space-time processing adds a new dimension to OFDM that can dramatically enhance some key operational parameters in a wireless network. In this chap-

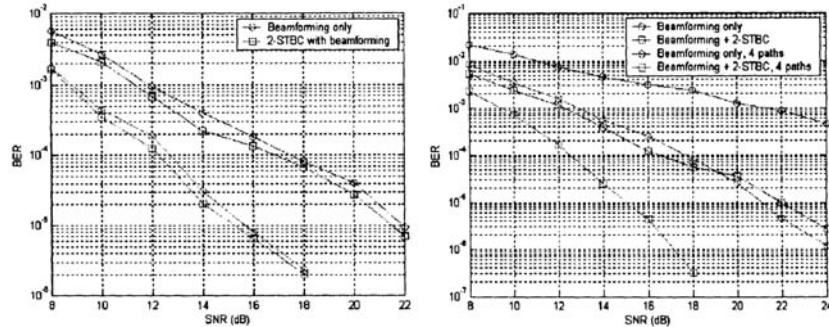


Figure 4.13: Beamforming with outer channel coding

ter, we discuss the basics of beamforming, space-time coding, the capacity of a MIMO system, and the use of STC/beamforming in OFDM systems. The activities in this area have led to many exciting breakthroughs, some of which have already been adopted into new wireless standards such as the WiFi and the WiMAX.

Appendix I: derivation of \bar{P}_e

Let $\mathcal{C} = \mathbf{A}^H \mathbf{W}(\mathbf{C} - \mathbf{C}^e)$, $d^2 = \|\mathbf{H}\mathcal{C}\|_F^2$, (4.19) then can be rewritten as

$$P_e \leq \exp(-d^2/4N_o)$$

Note d^2 can be expressed as

$$d^2 = \|\mathbf{H}\mathcal{C}\|_F^2 = \sum_{i=1}^m \mathbf{h}_i^H \mathcal{C} \mathcal{C}^H \mathbf{h}_i$$

where \mathbf{h}_i is the i th column of \mathbf{H} . Substitute $\mathcal{C} \mathcal{C}^H$ with its eigenvalue decomposition $\mathbf{U} \Lambda \mathbf{U}^H$, we have

$$d^2 = \sum_{i=1}^{N_r} \mathbf{h}_i^H \mathbf{U} \Lambda \mathbf{U}^H \mathbf{h}_i = \sum_{i=1}^{N_r} \mathbf{g}_i^H \Lambda \mathbf{g}_i = \sum_{i=1}^{N_r} \sum_{j=1}^L \lambda_j |g_{ij}|^2$$

Since \mathbf{U} is an orthogonal matrix and \mathbf{h}_i^H is a vector with i.i.d complex Gaussian elements, $\mathbf{g}_i^H = \mathbf{h}_i^H \mathbf{U}$ also has i.i.d complex Gaussian elements. Therefore, d^2 is the sum of $N_r \times L$ independent χ^2 random variables each with 2 degrees of freedom, and has the characteristic function as follows:

$$\psi_{d^2}(j\omega) = \left(\prod_{j=1}^L \frac{1}{1 - j\omega\lambda_j} \right)^{N_r}$$

Hence the average PEP is

$$\begin{aligned} \bar{P}_e &= \psi_{d^2}(j\omega)|_{\omega=\frac{-j}{4N_o}} = \left(\prod_{j=1}^L \frac{1}{1 + \frac{\lambda_j}{4N_o}} \right)^{N_r} \\ &\leq \left(\frac{1}{4N_o} \right)^{-N_r L} \left(\prod_{j=1}^L \lambda_j \right)^{-N_r} \\ &= \left(\frac{1}{4N_o} \right)^{-N_r L} |\mathcal{C}\mathcal{C}^H|^{-N_r} \\ &= \left(\frac{1}{4N_o} \right)^{-N_r L} |\mathbf{A}^H \mathbf{W}(\mathbf{C} - \mathbf{C}^e)(\mathbf{C} - \mathbf{C}^e)^H \mathbf{W}^H \mathbf{A}|^{-N_r} \end{aligned}$$

Appendix II: proof of proposition 5

For the STC only scheme, each codeword matrix has dimension $N_t \times N_t$. The average receiving SNR on the i th subcarrier is

$$\overline{SNR}_{STC} = \frac{1}{N_t} \frac{1}{N_r N_o} E \left\{ \text{tr} \left[\mathbf{H} \mathbf{D}_i \mathbf{A}^H \tilde{\mathbf{X}} \tilde{\mathbf{X}}^H \mathbf{A} \mathbf{D}_i^H \mathbf{H}^H \right] \right\}$$

where the factor $\frac{1}{N_t}$ is due to the fact that each codeword spans N_t time slots, and $\frac{1}{N_r N_o}$ is the total noise power on N_r receive antennas. With the assumption that $E \left\{ \tilde{\mathbf{X}} \tilde{\mathbf{X}}^H \right\} = \mathbf{I}_{N_t}$,

$$\begin{aligned} \overline{SNR}_{STC} &= \frac{1}{N_t} \frac{1}{N_r N_o} E \left\{ \text{tr} \left[\mathbf{H} \mathbf{D}_i \mathbf{A}^H \mathbf{A} \mathbf{D}_i^H \mathbf{H}^H \right] \right\} \quad (4.23) \\ &= \frac{1}{N_t} \frac{1}{N_r N_o} E \left\{ \text{tr} \left[\mathbf{H} \mathbf{D}_i \mathbf{U} \Sigma_+^2 \mathbf{U}^H \mathbf{D}_i^H \mathbf{H}^H \right] \right\} \\ &= \frac{1}{N_t} \frac{1}{N_r N_o} \sum_{l=1}^L \sigma_l^2 E \left\{ \text{tr} [\mathbf{h}_l'^H \mathbf{h}_l'] \right\} \\ &= \frac{1}{N_r N_o} (\sigma_1^2 + \dots + \sigma_L^2) \end{aligned}$$

where in the second step, we substitute \mathbf{A}^H with its SVD, $\mathbf{A}^H = \mathbf{U}[\Sigma_+ | 0] \mathbf{V}^H$; and in the third and the last steps, we use the facts that $[\mathbf{h}_1' \dots \mathbf{h}_L'] = \mathbf{H} \mathbf{D}_i \mathbf{U}$ has i.i.d complex Gaussian elements and $E \left\{ \text{tr} [\mathbf{h}_l'^H \mathbf{h}_l'] \right\} = N_r$.

For the STC-Beamforming scheme, the average receiving SNR is

$$\overline{SNR}_{STC-BF} = \frac{1}{L} \frac{1}{N_r N_o} E \left\{ \text{tr} \left[\mathbf{H} \mathbf{D}_i \mathbf{A}^H \mathbf{W}_i \mathbf{C}_i \mathbf{C}_i^H \mathbf{W}_i^H \mathbf{A} \mathbf{D}_i^H \mathbf{H}^H \right] \right\}$$

with a similar derivation as for the STC only scheme, it can be shown that

$$\overline{SNR}_{STC-BF} = \frac{1}{LN_o} (\sigma_1^2 + \dots + \sigma_L^2) \quad (4.24)$$

Comparing (4.23) with (4.24), we have

$$10 \log_{10} \left(\frac{\overline{SNR}_{STC-BF}}{\overline{SNR}_{STC}} \right) = 10 \log_{10} \left(\frac{N_t}{L} \right).$$

Appendix III: proof of proposition 6

Transmitting along the first right singular vector of the matrix \mathbf{A}^H , i.e., the dominant eigenmode transmission, is optimum in terms of receiving SNR. This is because all transmit energy is concentrated along the direction corresponding to the largest singular value (hence the largest gain). All we need to show is that with this beamformer, the outer channel coding across subcarriers can catch all the available diversity.

To show this, consider the composite channel seen by the outer channel coding. Substituting the beamformer matrix $\mathbf{w} = [\mathbf{w}_1]$ into the channel model, we have the composite channel for the i th subcarrier as

$$\begin{aligned} \hat{\mathbf{h}}_i &= \sigma_1 [\mathbf{h}_1 \cdots \mathbf{h}_L] \mathbf{D}_i \mathbf{u}_1 \\ &= \sigma_1 [\mathbf{h}_1 \cdots \mathbf{h}_L] \begin{bmatrix} e^{-j \frac{2\pi}{N} \tau_1 i} & & \\ & \ddots & \\ & & e^{-j \frac{2\pi}{N} \tau_L i} \end{bmatrix} \begin{bmatrix} u_{11} \\ \vdots \\ u_{1L} \end{bmatrix} \end{aligned}$$

where \mathbf{u}_1 and σ_1 are the first left singular vector and the largest singular value of matrix \mathbf{A}^H , respectively. Thus, the composite channel for the i th subcarrier is the sum of L uncorrelated Rayleigh fadings with different phase rotations. With the assumption that all L paths have different τ_l , these phase rotations are different across subcarriers.

Denote d_{\min} the minimum Hamming distance of the outer FEC code. We further assume that d_{\min} differences in coded bits result in d_{\min} different symbols after modulation mapping, which is almost the case when a bit interleaver exists between the encoder and the modulator. Following the similar PEP derivation as in Appendix I, the average PEP for the coded system can be shown as

$$\overline{P}_e = \left(\prod_{j=1}^r \frac{1}{1 + \frac{\lambda_j}{4N_o}} \right)^{N_r}$$

where $\lambda_1, \lambda_2, \dots, \lambda_r$ are the r nonzero eigenvalues of the correlation matrix $\mathbf{R}_{\hat{h}_s} = E \{ \hat{h}_s \hat{h}_s^H \}$, and \hat{h}_s is the composite channel vector at subcarriers $S = \{s_1, s_2, \dots, s_{d_{\min}}\}$, where two FEC codewords differ. Clearly, the rank of the correlation matrix $\mathbf{R}_{\hat{h}_s}$, r , determines the diversity order that the scheme can achieve.

The rank r can be determined by plugging (4.21) into the correlation matrix,

$$\mathbf{R}_{\hat{h}_s} = E \{ \hat{h}_s \hat{h}_s^H \} = E \{ \mathbf{B}_1 [\mathbf{h}_1 \cdots \mathbf{h}_L]_1^H [\mathbf{h}_1 \cdots \mathbf{h}_L] \mathbf{B}_1^H \} = \mathbf{B} \mathbf{B}^H$$

where

$$\begin{aligned} \mathbf{B} &= [\mathbf{D}_{s_1} \mathbf{u}_1 \quad \mathbf{D}_{s_2} \mathbf{u}_1 \quad \cdots \quad \mathbf{D}_{s_{d_{\min}}} \mathbf{u}_1] \\ &= \begin{bmatrix} u_{11} & & & \\ & \ddots & & \\ & & u_{1L} & \end{bmatrix} \begin{bmatrix} e^{-j \frac{2\pi}{N} \tau_1 s_1} & \cdots & e^{-j \frac{2\pi}{N} \tau_1 s_{d_{\min}}} \\ \vdots & \ddots & \vdots \\ e^{-j \frac{2\pi}{N} \tau_L s_1} & \cdots & e^{-j \frac{2\pi}{N} \tau_L s_{d_{\min}}} \end{bmatrix} \end{aligned}$$

Note that the second matrix in the above equation is nothing but a submatrix of an $N \times N$ DFT matrix. When the delay spread is uniform, it can be easily shown that the matrix is rank L , as any of its L columns form a Vandermonde matrix. In other cases, any L columns are shown to be almost always linearly independent. Hence the matrix is also rank L . Therefore, matrix \mathbf{B} , and consequently the correlation matrix $\mathbf{R}_{\hat{h}_s}$, is rank L as long as d_{\min} is larger than the number of the available paths L . This can be easily accomplished with an adequate FEC code.